Characterizing Heterogeneous Bacterial Surface Functional Groups Using Discrete Affinity Spectra for Proton Binding

ARTICLE *in* ENVIRONMENTAL SCIENCE AND TECHNOLOGY · NOVEMBER 1999

Impact Factor: 5.33 · DOI: 10.1021/es990627l

4 AUTHORS, INCLUDING:

Scott Smith
Wilfrid Laurier University
64 PUBLICATIONS **1,355** CITATIONS
SEE PROFILE

Lesley A. Warren
McMaster University
70 PUBLICATIONS **1,451** CITATIONS
SEE PROFILE

F. Grant Ferris
University of Toronto
151 PUBLICATIONS **6,639** CITATIONS
SEE PROFILE

Environ. Sci. Technol. **1999**, *33,* 4514−4521

Characterizing Heterogeneous Bacterial Surface Functional Groups Using Discrete Affinity Spectra for Proton Binding

JENNY S. COX,[†,‡] D. SCOTT SMITH,[†] LESLEY A. WARREN, AND F. GRANT FERRIS*

Department of Geology, University of Toronto, 22 Russell Street, Toronto, Ontario, M5S 3B1 Canada

Here we report results from a quantitative investigation of the types and densities of proton binding sites on a bacterial surface, *Bacillus subtilis*, from replicate acid−base titrations on bacteria at two ionic strengths (0.025 and 0.1 M). In contrast to the surface complexation modeling (SCM) approach developed and widely used for mineral, e.g., iron oxides, and more recently bacterial surfaces; we fit the data using the linear programming method (LPM). Our results using LPM indicate five discrete binding sites occurring on the surface of *B. subtilis* likely corresponding to carboxylic sites at low pK_a values, phosphoric sites at near-neutral pK_a values, and amine sites at high pK_a values. Replicate titrations on subsamples from the same bacterial population indicated less variability than has been suggested for bacterial surfaces. Both the pK_a and site density values were found to be dependent on ionic strength. Comparing the pK_a values determined here with LPM for *B. subtilis* to those determined independently by using a fixed three site SCM model shows excellent agreement with the common sites likely corresponding to carboxylic, phosphoryl, and amine groups. However, the LPM approach identifies a further two sites as compared to the SCM approach. These results have an important implication. Surfaces of a given bacterial strain have a quantifiable, characteristic geochemical reactivity reflecting discrete sites that can be traced back in terms of function to the underlying, cell wall structure, a well-characterized phenomenon for most bacteria. However, an important caveat of our findings is that the absolute densities of these sites are highly dependent on a suite of both microbiological and system chemical parameters.

Introduction

The overwhelming importance of interfacial reactions for controlling contaminant behavior in aqueous environments has focused attention on characterizing important solid surfaces with respect to functional groups and sorptive capacities. In particular, there has been considerable effort on mineral surfaces, such as iron oxides (*1*−*5*), and on natural organic matter (NOM), such as humic and fulvic acids (*6*−*9*). It is becoming increasingly recognized that bacteria are also abundant in aqueous environments and possess highly geochemically reactive surfaces (*10, 11*). As yet, there has been comparatively little work investigating bacterial surfaces, although there have recently been efforts to determine geochemically relevant information, such as types and densities of surface functional groups for bacteria. Recent works by Fein and co-workers (*11*−*13*) have interpreted metal and proton titrations of bacteria using surface complexation models (SCM) and FITEQL, which is often used for metal oxides. There are many approaches to surface complexation modeling in the literature. For natural organic matter (NOM), an approach that has achieved excellent results is the linear programming method (LPM) (*9*). In this paper, the LPM is tested as an alternative approach to traditional SCMs in modeling bacteria titrations.

Bacteria are classified as either Gram-positive or Gram-negative as distinguished by the Gram stain (*14*). This classification divides bacteria into two main groups that differ in their cell wall characteristics and, thus, most likely their geochemical reactivity as well. Gram-positive bacteria have a simple cell well wall consisting entirely of peptidoglycan, an amino sugar polymer, with attached teichoic and teichuronic acids (*15, 16*). Gram-negative bacterial surfaces are more complex, containing an external outer membrane that overlies a thin layer of peptidoglycan. This outer membrane consists of proteins, phospholipids, and lipopolysaccharides (*17*). In general, Gram-positive bacteria likely have a greater sorptive capacity due to their thicker layer of peptidoglycan, which contains the major sorptive sites. Bacterial surfaces consist of a complex, heterogeneous mixture of potential binding sites for metal and protons. The types of sites available include carboxylic, phosphoric, phosphodiester, amino, and hydroxyl groups (*18*); there can be significant overall variability in the relative numbers of these surface sites among bacteria. This variability is a result of several factors: differences in cell wall structure and hence types and densities of surface functional groups among bacterial strains; the inherent heterogeneity of the bacterial cell wall, which is compounded by effects of growth media, cell metabolic state, and age for any given bacterial strain; and solution compositional effects that can further influence the bacterial surface characteristics.

The aforementioned differences due to cell metabolic state and growth medium occur because bacteria are living organisms that rely on diffusion for both their nutrient supply and waste removal, and thus necessarily, they have evolved active transport mechanisms to move elements across their cell membrane (*10*). Their surface charge is therefore not simply passively dependent on solution chemistry but is also actively affected and controlled by cell metabolic processes. For example, actively respiring *Bacillus subtilis* cells pump protons to the cell wall, which reduces the surface's capacity to bind metal ions because protons occupy the metal binding sites (*19*). In addition, the nature of the growth media affects the types of surface groups developed and thus sorptive capacities, even within the same bacterial strain. For example, the relative abundance of teichoic and teichuronic acids occurring as part of the cell surface peptidoglycan layer of *Bacillus subtilis*, a Gram-positive bacteria, is dependent on P, Mg, and Na concentrations (*20*). Thus, if nutrients such as P are limiting, the structure of the cell wall may be affected. The geochemical relevance of this lies in the pK_a value of these acids. Teichoic acids are phosphate-containing polymers that are covalently bound to the peptidoglycan of the cell wall, while teichuronic acids are linear polysaccharides

* Corresponding author email: ferris@quartz.geology.utoronto.ca; fax: (416)978-3938; tel: (416)978-0526.

† Joint first authors.

‡ Present address: Institut für Mineralogie und Petrographie, ETH-Zentrum, CH-8092 Zürich, Switzerland.

10.1021/es990627l CCC: $18.00
Published on Web 11/04/1999

that contain uronic residues (*20*). If teichuronic acids dominate, then carboxylic sites will more abundant (pK_a ~4−6); whereas if teichoic acids dominate, then phosphoric (pK_{a1} ~0.2−2.91, pK_{a2} ~ 5.6−7.2) and phosphodiester sites (pK_a ~3.2−3.5) would be expected to be more abundant. The relative sorptive capacity of the bacteria will be very different depending on which type(s) of sites dominate.

Bacterial surfaces are more variable and heterogeneous than mineral surfaces precisely because of the aforementioned factors. There are two fundamental types of heterogeneity, one due to the inherent variability of the cell wall structure and another due to the influence of metabolic state and growth conditions. These two sources of variability cannot be separated, and any experimental approach to investigate bacteria surface reactions must allow for their overall heterogeneity. For this reason, such studies will reflect operationally defined quantities that are dependent on the conditions of the experiments.

To probe the nature of surface sites on bacteria, it is possible to use acid−base titrations. The surfaces sites are perturbed by the addition of titrant, and the effect can be observed using a glass electrode to measure the free hydrogen ion concentration. However, this approach is only valid provided that the culture of the bacteria as well as the titrations themselves are carefully controlled to minimize induced changes in bacterial surface site characteristics. The resulting titration curve can be interpreted by some model for the system. Such acid−base titrations are routinely used to characterize mineral surfaces (*21*−*24*), and the resultant titration curves are often fitted to a model using programs such as FITEQL (*25*). Often models for proton binding to mineral surfaces contain a fixed number of presupposed reactions, such as "two p*K*" models (*26*). This approach is limited for bacteria because of the variability of their surface sites. There have been numerous proposed methods to model proton interactions with heterogeneous sorbents, such as NOM and natural colloids. These have been summarized by Perdue (*27*) and fall into continuous and discrete approaches, where continuous approaches represent proton binding by a continuum of binding sites and discrete methods approximate this continuous function by a few discrete sites.

Titration data can be modeled as distinct sites by determining the minimum number of sites to achieve a good fit to the data. In this approach, both the acidity constants and site densities for each site are fit to the data, and the number of sites are increased until a sufficiently good fit to the data is achieved. This is the approach used in FITEQL and is commonly applied to simple iron oxide titration data (*2*, *28*) and has recently been applied to bacteria (*11*−*13*). An alternative approach is to fix the acidity constants and fit only the ligand concentrations, resulting in a pK_a spectrum (*6*, *9*, *29*−*33*). The pK_a spectrum method determines the minimum number of components necessary to describe the data. Thus, it is not necessary to assume the number of sites before fitting the data. The flexibility of this approach is advantageous for modeling bacterial surfaces as there are likely a continuum of acidity constants reflecting subtle variations in cell surface characteristics rather than two or three simple discrete sites.

Proton binding is dependent on ionic strength, and there are numerous proposed methods to investigate electrostatic effects in proton binding (*7*, *34*, *35*). The simplest methods add terms in the optimization routine that attempt to describe electrostatic effects. These are typified by the constant capacitance (*36*) and Stern models (*37*). These models have been criticized in that the parameters are not necessarily independent, and many different sets of parameters can lead to equivalent descriptions of the data (*38*).

It is possible to separate the fitting problem into two subproblems, one to address electrostatic effects and another to address chemical heterogeneity. The first step is to remove electrostatic effects by decomposing titration curves at different ionic strengths into one so-called master curve (*35*). The second problem is to fit the master curve with an equilibrium speciation model. This approach has been applied for bacterial cell walls at three salt levels (*39*). Although this approach is very attractive, there is no accepted model for electrostatic behavior of humic substances (*7*), and even less work has been performed for bacterial surfaces. In addition, electrostatic models need various simplifying assumptions, such as planarity, that are likely not true for bacterial surfaces. It is known that charge is not evenly distributed on the cell walls of bacteria (*20*).

A simpler approach is adopted here. The results of titrations of *Bacillus subtilis* at two ionic strengths are fit separately to pK_a spectra without any attempt to model electrostatic terms. Thus, the results are conditional on ionic strength, and the stability constants determined are not intrinsic constants but rather are apparent constants. To control as much as possible the variability caused by the metabolic state of the bacteria, these titrations were performed on live bacteria that were not actively growing, and the viability of the bacteria was tested throughout the titrations.

Materials and Methods

Growth of Culture. *Bacillus subtilis* cells for titrations were harvested from pure cultures grown in brain and heart infusion (BHI, Becton Dickinson, Cockeysville, MD), shaken gently at 30 °C for 15−16 h. Viability and growth phase of the cells were examined by microscopy before use and spot-checked during and after the titration. Cell viability was evaluated by performing live/dead direct cell counts using epifluorescence microscopy and the live/dead Baclight bacterial viability kit (Molecular Probes Inc.).

Preparation of Cells for Titration. *Bacillus subtilis* cells were recovered from the growth media by sterile transferral to an acid-washed, autoclaved centrifuge bottle that was centrifuged at 7000 rpm for 10 min. The broth was decanted, and the cells were resuspended in 100 mL of sterile 18 MΩ water. After further centrifuging at 7000 rpm for 10 min, the water was decanted, and the cells were resuspended in 100 mL of a sterile 0.001 M EDTA solution, soaked for 30 min, and then centrifuged under the same conditions listed above. After centrifugation, the EDTA solution was decanted; the cells were resuspended in 100 mL of the selected concentration of sterile $NaNO_3$ solution and centrifuged again. The $NaNO_3$ resuspension was repeated a second time, and the cells were finally resuspended a third time in 250 mL of the selected $NaNO_3$. All of the steps above were performed under sterile conditions with acid-washed, sterile plasticware and solutions.

We found experimentally using the BacLight live/dead stain and epifluorescence microscopy that the 30-min 0.001 M EDTA soak was effective in "cleaning" the bacterial surfaces of residual metals without affecting cell viability.

Solutions. All solutions used in this experiment were carefully prepared to be metal-free, sterile, O_2 and CO_2 degassed, and of analytically known concentrations. All plastic and glassware were soaked first for 24 h in 10% (v/v) trace metal grade nitric acid (Fisher) and then soaked for 48 h in 18 MΩ water. All solutions were prepared using sterile 18 MΩ water. To prevent contamination of the titration aliquot by the titrant or electrolyte solutions, all solutions were additionally sterile filtered after preparation to remove any potential trace microbial contamination, and all plasticware was either autoclaved or, where this was not possible, disinfected with 80% EtOH. Solutions were also checked under the microscope to confirm sterility.

Solutions were degassed for 20 min with 99.998% N_2, using sterile, disposable plastic pipets and kept in an anaerobic chamber when not in use to keep out O_2 and particularly CO_2, which would affect the pH. The titrant solutions and titrant aliquot were also degassed again immediately prior to titration and kept under positive pressure of N_2.

The $NaNO_3$ solutions were prepared by weighing out a known amount of $NaNO_3$ (Sigma, SigmaUltra grade) using an analytical balance and preparing the solution using volumetric flasks of known tolerance. The concentrations of $NaNO_3$ used in this experiment were 0.02532 ± 0.00001, 0.09879 ± 0.00004, and 0.09920 ± 0.00005 M. There were no systematic differences in the titrations with a nominal ionic strength of 0.1 M, so these experiments were pooled for data analysis. The ethylenediaminetetraacetic acid solutions were similarly prepared with EDTA from Sigma (SigmaUltra grade).

The NaOH solution was prepared according to the standard analytical method (40): an approximately 0.1 M solution was prepared from a 50% NaOH solution (NaOH from Sigma, SigmaUltra grade) and sterile, degassed 18 MΩ water and then standardized by titration under a positive pressure of nitrogen against an analytically known weight of dried KHP (Fisher, ACS grade). The HCl titrant solution was prepared by dilution of trace metal grade 37% HCl (Fisher, Trace grade) in 18 MΩ water. The exact concentration was determined by titrating against the standardized NaOH. Four titrations were performed with a relative standard deviation of 0.3%; the final NaOH concentration was determined to be 0.1795 ± 0.0006 M. The HCl titrant solution was prepared by dilution of trace metal grade 37% HCl (Fisher, Trace Grade) in 18 MΩ water. The exact concentration was determined by titrating three 10-mL aliquots against standardized NaOH; the three runs had a relative standard deviation of 0.04%, and with the inclusion of propagated error, the final concentration of HCl was determined to be 0.336 ± 0.002 M.

Titrator Settings. All titrations were preformed in a glass vessel with lid as part of a Metrohm GP 736 Titrino unit interfaced by Titrino Workcell v3.1 software to a personal computer. Two separate buret exchange units with 20-mL burets were used, one for acid and one for base. We also used a Metrohm titrator vessel lid (part no. 6-1414-010) with a gas line interface of our own construction. Temperature was recorded by an interfaced thermocouple resting in water at the current room temperature; the error of the temperature probe was ±0.1 °C. The electrode was three-point calibrated with fresh buffer before each experiment (pH 4, 7, and 10), and the slope was consistently 99% of the Nernst value.

The details of the instrument parameters are of crucial importance to the accuracy of the results, so we present them here in full. For live cell titration, our Titrino unit was programmed with a "monotonic equivalence point titration" (MET) method, which adds the same volume of titrant at each step. This was found to greatly increase the resolution over a dynamic titrating method without the introduction of 'ghost' equivalence points. The MET method is as follows: after an initial pause of 10 s, 6 μL of titrant was added; when the signal drift reached 10 mV/min, another 6 μL of titrant was added; and this process was repeated until the titration was halted when the pH reached either 2.9 or 10.9. For the range of data used (pH 4−10), the titration method yielded data points in approximately equal pH intervals.

Titration of Bacteria. The titrator electrode was first calibrated as mentioned above. The optical density ($OD_{600\ nm}$) of the stock bacterial suspension in $NaNO_3$ electrolyte was measured prior to each titration run. The measured absorbance was compared to a prepared calibration curve to determine the concentration of bacteria (mg/L). The absorbances used were in the range of 0.66−0.96, which corresponds to 0.67−0.98 mg of bacteria/L. A known volume of aliquot, approximately 50 mL, was then transferred in a sterile fashion to the titration vessel, which was immediately attached to the lid setup attached to the N_2 gas line. A sterile Teflon magnetic stir bar was also added to the vessel at this step. The titrant bottles were also hooked up to the gas line. The entire system was then degassed for 5−7 min. Longer times were found to be unnecessary since the titrant aliquot was small, and the titrant solutions were previously degassed. A positive pressure of N_2 was then maintained by allowing a gentle flow of N_2 through the entire system during the titration.

The bacterial aliquot was then quickly titrated to a pH value of 2.9, the buret exchange unit was then changed, and the titration of the aliquot with NaOH up to pH 10.9 was begun. Total time for each titration was approximately 45 min. Note also that the buret tip was cleaned and disinfected prior to insertion into the titration vessel.

The pH sequence 'down−up' was carefully chosen after tests revealed a higher tolerance of *B. subtilis* to acid over base. When the bacteria were titrated first 'up' in pH and then 'down' in pH, viability was compromised, and many cells were found to be dead. However, a titration 'down−up' in our choice of pH range did not seem to affect the viability of the cells; they were found by the BacLight test to be >90% alive at the end of the titration. For this reason, all live cell titrations were performed in this sequence.

Data Analysis. The titration data were analyzed using the linear programming method (LPM) proposed by Brassard et al. (*31*). A full discussion can be found in Brassard et al. (*31*), but a brief discussion is given here. This method has been applied successfully to kaolinite titrations (*21*) and for NOM titrations (*9*). All data analysis was performed using Matlab (The MathWorks Inc.), and all calculations are based on concentrations. Measured pH values were determined by comparison to the NIST activity standards (pH 4, 7, and 10) and converted to $[H^+]$ using the Davies equation (*41*). The nominal ionic strengths are as reported below, but the actual ionic strength was calculated at each addition of titrant in order to calculate $[H^+]$.

The linear programming method assumes that a heterogeneous mixture of binding sites, such as on bacteria surfaces, can be treated as a sum of n monoprotic sites. For the jth addition of acid or base, the charge balance expression can be written (*31*)

$$C_{bj} - C_{aj} + [H^+]_j - [OH^-]_j = \sum_{i=1}^{n}\left(\frac{L_{Ti}K_i}{K_i + [H^+]_j}\right) - \mathrm{ANC} \quad (1)$$

where C_{bj} and C_{aj} correspond to concentrations of base and acid for the jth addition of titrant, and ANC corresponds to the initial acid-neutralizing capacity of the system. For the ith site, the acidity constant is K_i, and the ligand concentration is L_{Ti}. In this model, the terms on the left can be estimated using experimental data, and the terms on the right are the fitting parameters.

Equation 1 could be solved by setting the number of sites (n) and varying both L_{Ti} and K_i. This is essentially what FITEQL does, where n is increased until the fit is good enough. To avoid selecting n and to prevent convergence problems caused by the correlation of L_{Ti} and K_i, it is preferable to fix the pK_a values as a grid from a minimum to a maximum value at fixed step sizes. The ligand concentration associated with each pK_a value is assigned a positive value where zero is a possible result; the result is the so-called pK_a spectrum. In using a pK_a spectrum method, the necessary number of sites is selected as all the pK_a values having a nonzero concentration. In general, the minimum and maximum pK_a correspond respectively to the minimum and maximum measured pH. For the experiments here, the pK_a grid was defined from 4 to 10 in steps of 0.2. This pH range was selected

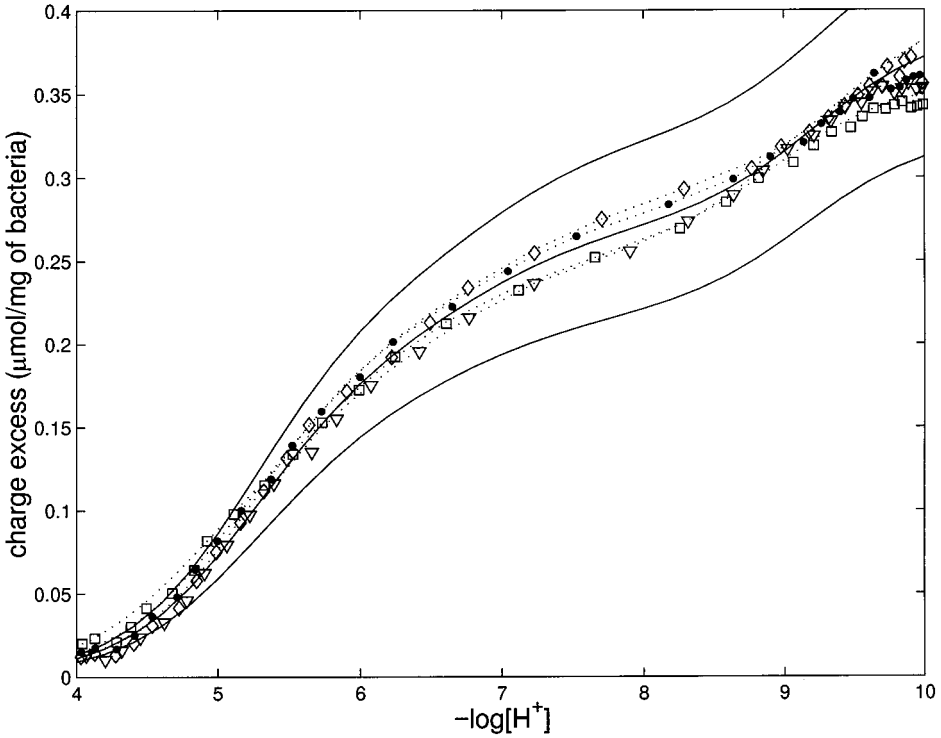

FIGURE 1. Charge excess versus −log[H^+] for four replicate acid−base titrations of *Bacillus subtilis* from the same population at an ionic strength of 0.025 M ($NaNO_3$). Each symbol corresponds to the data for one titration. The dotted lines are the best-fit lines for each data set individually. The solid lines correspond to the five site model obtained by pooling the individual results ± one standard deviation (see text).

because Smith et al. (*33*) demonstrate that errors for acid−base titrations outside this range are very large. There may be sites outside this range, but they are difficult to observe using a glass electrode. In addition, sites outside this range are not environmentally significant because at pH values observed for natural waters (~4−9), the weak proton binding sites will be fully dissociated, and the strong proton binding sites will be fully protonated.

Once the pK_a values are selected, the matrix version of eq 1 is setup as $\mathbf{Ax} = \mathbf{b}$. Where the matrix $\mathbf{A}$ is an $m \times n$ matrix of α terms, where the entry at the ith column and jth row for n proposed sites and m additions of titrant is

$$\alpha_{ij} = \frac{K_i}{K_i + [H^+]_j} \quad \text{for } i = 1 \ldots n \text{ and } j = 1 \ldots m \qquad (2)$$

The unknown $n \times 1$ vector, $\mathbf{x}$, contains the ligand concentrations for each of the m sites. The $m \times 1$ vector $\mathbf{b}$ contains the measured charge excess ($C_b - C_b + [H^+] - [OH^-]$), for each of the m titration points. Traditional least-squares cannot be used to solve the matrix equation because the results must be positive. It is possible to use least-squares solution only if constrained optimization ($\mathbf{x} \geq 0$) is used. This has been done using regularized least-squares techniques (*6*, *32*).

Smith et al. (*33*) have shown that linear programming tends to reduce the number of sites as compared to constrained least-squares optimization. Although least-squares regularization for a small number of sites could be used (*6*), here we use linear programming to solve the matrix equation $\mathbf{Ax} = \mathbf{b}$, as the linear programming solution minimizes based on the absolute of the error, which tends to emphasize zero as a solution and to emphasize peaks (*9*). This avoids the convergence problems in FITEQL where the solution is sometimes a local rather then a global minimum (*38*). In fact, in the LPM there is only one minimum, which is the global minimum. The matrixes to solve the linear programming problem were setup as in Brassard et al. (*31*) and solved using the Matlab linear programming routine (*42*).

Results and Discussion

Cell viability was evaluated at the beginning of the experiments as well as during titrations and at the end by direct cell counts using epifluorescence microscopy and the BacLight molecular probe. Using the pH "down−up" titration sequence, no significant effect on cell viability was observed. Viable cell counts at the beginning of titrations were ~95% live, and at the end of the experiment the bacteria were still >90% live. This demonstrates that the bacteria were still alive during the titrations. In addition, it must be assumed that the treatment of the bacteria before the titration, such as the osmotic shock of taking them from their growth media to ultrapure water, does not change their physiology. This assumption is necessary if the fitting results for these experiments are going to apply to naturally occurring bacteria.

Figures 1 and 2 show the titration curves for live, metabolically inactive *B. subtilis* cells after transformation to the charge balance expression (eq 1) for four titrations at 0.025 M (Figure 1) and six titrations at 0.1 M ionic strength (Figure 2). It can be seen that the data occur in approximately equal pH steps, which is a requirement of the LPM (*31*) so that no sites are assigned preferential weight in the fitting routine. Each individual titration curve shows little variability about the best-fit line. There is somewhat greater variability among titrations at a given ionic strength but still consistent trends are observed for the titration curves in each set. These results demonstrate that while some surface variability can occur with the same bacterial strain, analogous to aging or subtle preparatory differences for minerals solids, reproducible quantitative titration curves for estimates of surface characteristics can be made.

Comparison of Figures 1 and 2 reveals that the shape of the titration curve is a function of ionic strength. The most

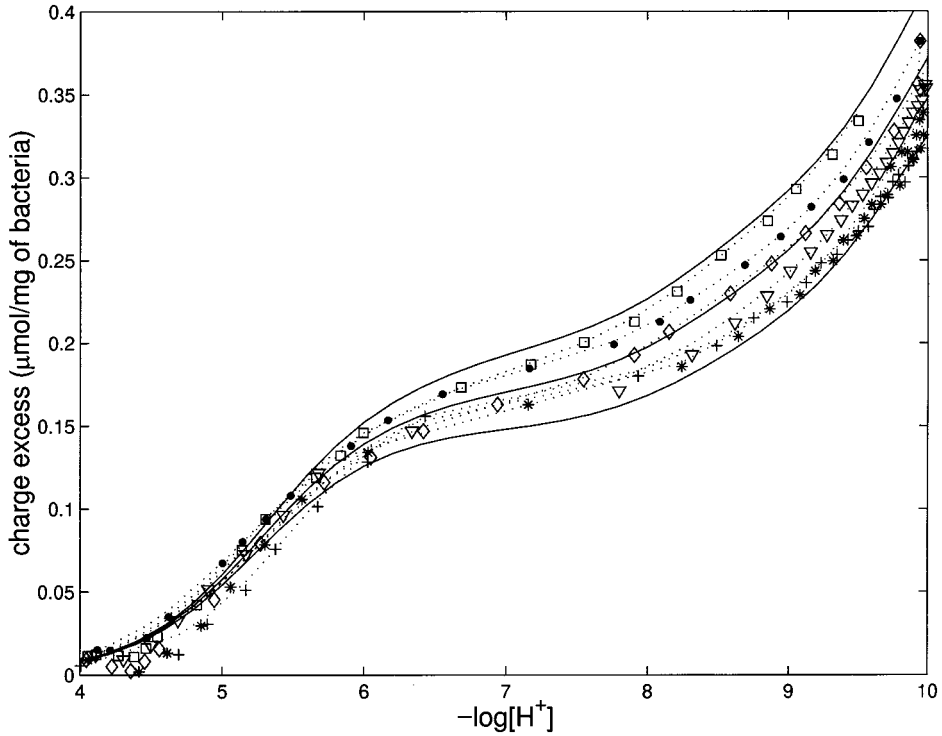

FIGURE 2. Charge excess versus −log[H$^+$] for six replicate acid−base titrations of *Bacillus subtilis* from the same population at an ionic strength of 0.1 M ($NaNO_3$). Each symbol corresponds to the data for one titration. The dotted lines are the best-fit lines for each data set individually. The solid lines correspond to the five site model obtained by pooling the individual results ± one standard deviation (see text).

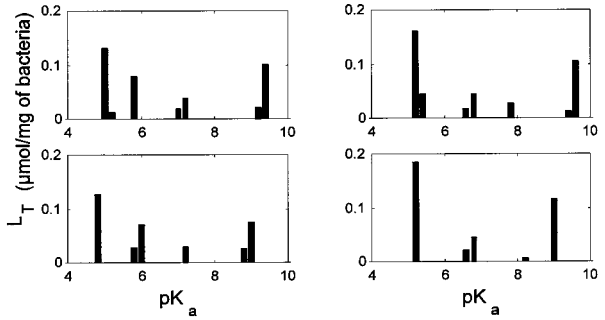

FIGURE 3. pK_a spectra determined for *Bacillus subtilis* using the LPM method for 0.025 M titrations. Each plot corresponds to one of the replicate titrations ($n = 4$).

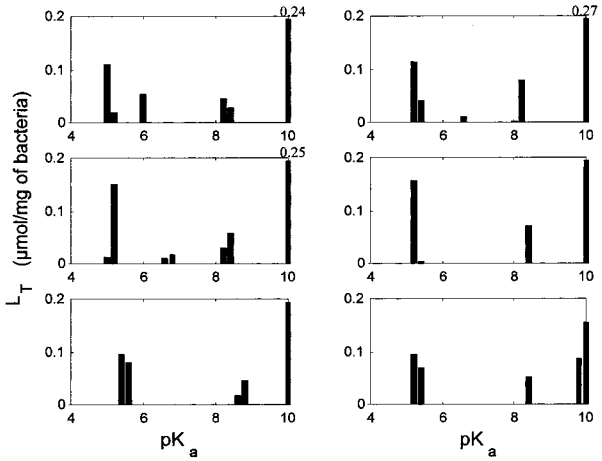

FIGURE 4. pK_a spectra determined for *Bacillus subtilis* for 0.1 M titrations. Each plot corresponds to one of the replicate titrations ($n = 6$).

prominent difference is the large upward trend at the basic end of the titration for the 0.1 M ionic strength titration; whereas, the lower ionic strength titration starts to reach a plateau at the basic end of the titration. However, the total excess charge is very similar by the end of both titrations, with values around 0.35 μmol/mg of bacteria. This result demonstrates that first the proton binding to bacterial surfaces is ionic strength dependent and, second, the effect is more pronounced at higher pH as the ligand sites on the bacteria acquire a negative charge.

The pK_a spectra resulting from fitting the data from replicate titrations using LPM at the two ionic strengths (0.025 and 0.1 M) are shown in Figures 3 and 4, respectively. Overall there are clusters of ligands with acidity constants around 5, 7, and 9 for 0.025 M titrations and around 5, 8.5, and 10 for the 0.1 M titrations. For the lower ionic strength titrations, there are also some peaks around a pK_a value of 8. The higher ionic strength titration has a smaller cluster of peaks just below a pK_a value of 7. From the clustering of peaks in the pK_a spectra, five average sites were selected to represent the data for both sets of titrations. A summary of these proposed ligand classes along with the number of titrations represented in each class is given in Table 1. Variability in bacteria surface

TABLE 1. Ligand Classes Identified from Titrations of *Bacillus subtilis*

site	pK_a range	number of occurrences[a] $I = 0.025$ ($n = 4$)	$I = 0.1$ ($n = 6$)
1	4.8−5.6	4	6
2	5.8−6.4	2	1
3	6.6−7.6	4	2
4	7.8−8.6	2	6
5	8.8−10	4	6

[a] The number of occurrences refers to the number of titrations that include a peak in the indicated pK range. A perfect score for the first column is four and for the second column it is six.

TABLE 2. Acidity Constants (pK_a) and Site Densities for Five Proposed Sites on *Bacillus subtilis* Conditional on Ionic Strength at 0.025 and 0.1 M

	pK_a/L_T (μmol/mg of bacteria)[a]		
site	$I = 0.025$ M[b]	$I = 0.1$ M[b]	$I = 0.1$ M[c]
1	5.17 (0.01)/0.17 (0.04)	5.25 (0.03)/0.16 (0.02)	4.8 (0.1)/0.12 (0.01)
2	5.88 (0.01)/0.05 (0.05)	6.00 (0.00)/0.01 (0.02)	na
3	6.91 (0.05)/0.05 (0.02)	6.69 (0.01)/0.01 (0.01)	6.9 (0.3)/0.04 (0.02)
4	7.88 (0.04)/0.01 (0.01)	8.33 (0.01)/0.07 (0.01)	na
5	9.24 (0.07)/0.12 (0.01)	9.95 (0.06)/0.25 (0.03)	9.4 (0.3)/0.062 (0.02)

[a] Parentheses indicate one standard deviation. [b] From results presented here using LPM. Note, these are apparent constants. [c] From Fein et al. (*11*) where pK_a are intrinsic constants determined by a constant capacitance model using FITEQL.

TABLE 3. Proton Binding Sites in Bacteria

site	portion of cell wall	range of values
carboxylic	peptidoglycan (peptide and muramic acid residue parts) teichuronic acids	2−6 (mean 4.5)[a]
phosphodiesters	teichoic and linkage of teichuronic acids to peptidoglycan	3.2−3.5[b]
phosphoric	teichoic acid	0.2−2.91 (pK_{a1})[c] 5.65−7.20(pK_{a2})[c]
amines	peptidoglycan (peptide part)	9.0−11.0[d]
hydroxyl	peptidoglycan (muramic acid residue and possibly on peptide part) teichoic and teichuronic acids	8−12 (mean 10) phenolic[a] 12−13 monosaccharides[a]

[a] From ref *43*. [b] From ref *44*. [c] From seven phosphoric ligands in Martell and Smith (*45*). [d] From ref *15*.

functional groups is demonstrated in that some pK_a classes are only represented by one or two titrations. There is no way to distinguish true bacterial surface heterogeneity from preparation differences or experimental errors. Thus, the variation of the position and height of peaks determined from multiple titrations serve as an overall estimate of the error for replicate bacteria titrations.

The selection of five sites to represent the data is somewhat arbitrary. It would be possible to represent the data with fewer sites, but what is desired is an estimate of all of the possible sites, even the sites that are not represented in every titration. The effort here is not only to model the data but to also get an idea of structural variability between bacteria titrations and functional group information for bacteria surfaces. This type of classification approach has been used before to compare NOM from different sites in Norway (*9*).

To quantify this error and develop a five site model for proton binding to bacteria, the standard deviation and average pK_a and L_T were determined for each proposed site. From these ligand classes (Table 1), the mean pK_a values were determined using a weighted average, where the weighing factors were the associated ligand concentrations. Similarly, a weighted standard deviation (see ref *47*) was calculated to determine an approximate confidence interval about the pK_a value. For the ligand concentrations, the mean and standard deviation were calculated as the sum of concentrations in the ranges identified in Table 1. This approach to estimating uncertainty about proton binding parameters has not been used before. This method is advantageous in that it allows an overall estimate of uncertainty including experimental errors as well as systematic variation in sample preparation and inherent heterogeneity of bacterial cell walls. The fact that errors in acid−base titration curves are not random but rather show systematic trends (*33*) means that traditional error estimate methods cannot be applied and emphasizes the need for replicate titrations.

The five site model results are shown in Table 2. The most strongly acidic sites determined here have pK_a values of 5.17 and 5.25 for the 0.025 and 0.1 M ionic strength titrations, respectively. These sites are in the range of values determined for model carboxylic compounds (pK_a 2−6, mean 4.5), see Table 3. Also, site 2 in Table 1 could be interpreted as carboxylic, with pK_a values of 5.88 and 6.00 for the low and high ionic strength titrations, respectively. The third site in Table 2 has pK_a values near neutral, with values of 6.91 and 6.69 for the two sets of titrations. The near-neutral pK_a values are generally ascribed to phosphoric sites (*11*). More basic pK_a values are observed for the last two sites in Table 2. These sites have values from 7.88 to 9.95, which are similar to phenolic sites (pK_a 8−12, mean 10) or amines (pK_a 9−11), see Table 3. There are no pK_a values corresponding to carbon dioxide (6.3 and 10.3) because CO_2 was constantly scrubbed using nitrogen, so even if it were generated by respiration of the bacteria it would not be observed in the titration curve.

The solid lines in Figures 1 and 2 correspond to the five site models given in Table 2. The middle line is determined using the mean values reported in Table 2 for acidity constants and ligand concentrations. The upper and lower solid lines are determined using the mean value ± one standard deviation, respectively. In both Figures 1 and 2, it can be seen that the solid lines bracket the experimental observations very well in that most data points are included inside the confidence envelope; however, there are points outside the envelope by up to 0.02 μmol/mg at the lower pH values for both sets of titrations. Additionally, the envelope overestimates the error at upper pH values for the 0.025 M ionic strength titrations by about 0.04 μmol/mg of bacteria. The envelope is largest at the more basic end of the titration because the overall uncertainty at any point in the titration curve has additive contributions from all of the more acidic ligands.

The parameter values determined here are dependent on ionic strength. For the 0.025 and 0.1 M ionic strength titrations, the pK_a values are very similar for the three most acidic sites, with differences less than or equal to 0.2 of a log unit. The two more basic sites have stability constants that differ by 0.45 and 0.71 log unit with the higher ionic strength titration showing the greater divergence. The three most acidic sites have approximately the same concentrations, within error, for the low and high ionic strength titrations. The two strongest proton binding sites show higher apparent ligand concentrations in the higher ionic strength titration, with values of 0.1 versus 0.7 and 0.12 versus 0.25 μmol/mg

for the low and high ionic strength titrations, respectively. In general, the stability constants and ligand concentrations for the 0.025 and 0.1 M titrations are more similar at the acidic end of the tiration, and the 0.1 M titration produces larger values at the basic end of the titration. This is consistent with the observation that the 0.1 M titration curves (Figure 1) increase more sharply at high pH than the 0.025 M titration curves (Figure 2). The total site concentration, obtained by summing the concentration of all of the ligands, is very similar for the 0.025 and 0.01 M ionic strength titrations with values of 0.4 and 0.5 μmol/mg, respectively. This result demonstrates that, although the pK_a values shift in response to changes in ionic strength, the total concentration of proton binding sites available does not dramatically change; as is assumed in SCM models where electrostatic terms modify the pK_a values and not the ligand concentrations (*2, 36*).

Acid−base titrations do not give direct evidence of the nature of the proton binding sites, but it is possible to infer types of sites from comparison with pK_a values for model compounds. Possible functional groups in *Bacillus subtilis* are given along with pK_a ranges and location within the macromolecular structure of the bacterial cell wall in Table 3. Very acidic sites, such as some carboxylic groups, first dissociation of phosphoric sites, and phosphodiesters would not be observed in the titration range presented here. The usual interpretation is that the high pK_a sites (pK_a ∼10) are hydroxyls (*11*). For many bacteria, these are likely better interpreted as amine sites. Hydroxyl sites with pK_a values around 10 occur only for phenolic sites, at least in model compounds (*43*). Thus, unless the structure of the bacteria includes phenolic protons, it is more likely that high pK_a sites are amine groups. For example, sugar alcoholic protons have a pK_a value much higher (pK_a ∼12) than that attributed to phenolic protons (pK_a ∼10).

The parameters determined here can be compared with what is known about the structure of the cell wall for *Bacillus subtilis*. The proposed structures for peptidoglycan and teichoic acids in *Bacillus subtilis* (*18*, *20*) do not contain phenolic protons; so for the experiments performed here, the basic sites are better attributed to amine groups. The peptide portion of peptidoglycan has amines groups, and a survey of amino acid acidity constants in Smith and Martell (*45*) shows that secondary or primary amines have pK_a values in the range of 9−11 as reported in Table 3. Also, the peptide portion of peptidoglycan has carboxylic groups that could have pK_a values in range of 2−6 but often occur at much lower values (1.71−2.63) in isolated amino acids (*15*). These very acidic carboxylic groups would not be observed here because they fall outside of the analytical window of these titrations. The teichoic acids attached to the peptidoglycan include phosphodiester groups throughout the chain and a phosphoric group at the end. The pK_a values for the phosphodiesters would not be observed in the pH range here because they occur at values less than four. The terminal phosphoric groups would be observed because their values fall in the middle of the titration range. In summary, the sites that were observed here likely correspond to carboxylic for site 1, carboxylic or phosphoric (pK_{a2}) for site 2, phosphoric (pK_{a2}) for site 3, phosphoric (pK_{a2}) or amine for site 4 and amines for site 5.

The exact nature of the binding sites depends on the sources of variation mentioned above. The specific stereochemistry about each protolyte would be influenced by cross-linking of the peptide chains (*46*) as well. Thus, it is not possible to uniquely define each of the proposed five sites with a proposed molecular identity, although it can be said that the values determined here are reasonable given the structure of the cell wall for *Bacillus subtilis*. These results show that the acid−base titration curve for *B. subtilis* can be represented by five average sites, but they do not imply that there are only five possible sites in the cell wall structure of the bacteria.

The relative site densities show almost equal "carboxylic" and "amine" protons. This is reasonable because each peptide chain has an almost one to one occurrence of NH_3^+ and COOH groups, as demonstrated by the proposed structure of peptidoglycan (*18*). The lowest concentration is observed for the phosphoric groups, which is also consistent with known *B. subtillus* characteristics, as these will only be observed if the groups are terminal.

The results of Fein et al. (*11*) determined using acid−base titrations of *B. subtilis* and fit using a constant capacitance model in FITEQL (*25*) are included in Table 2 for comparison with the results determined here. Overall, the parameters reported by Fein et al. are consistent with the results presented here, except they allow only three sites in their modeling. The three sites that are most similar with the results presented here can be compared. The most acidic sites have pK_a values of 5.17 and 5.25 for the 0.025 and 0.1 M ionic strength titrations presented here as compared to 4.8 determined by Fein et al. (*11*). Similarly, for the near-neutral pK_a sites, the values are 6.91 and 6.69 here and 6.9 from Fein et al. (*11*). For the most basic site, the values are 9.24 and 9.95 here and 9.4 determined by Fein et al. (*11*). Overall, the acidity constants are within 0.5 of a log unit of each other, with the 0.025 M agreeing more closely with the results of Fein et al. than the 0.1 M ionic strength titration. In particular, the weakest acidic site (pK_a >9), where ionic strength effects are strongest, reveal the greatest differences, with pK_a values 0.16 and 0.55 log unit different from Fein et al. for the 0.025 and 0.1 M titrations, respectively. This is an explainable discrepancy because Fein et al. report constants extrapolated to zero ionic strength, whereas the constants determined here are at 0.025 and 0.1 M ionic strength, so it should be expected that the lower ionic strength titration would more closely resemble the "zero" ionic strength titration of Fein et al. (*11*). The total site density determined by Fein et al. (*11*) is about half the value determined here with a value of 0.222 μmol/mg versus 0.4 and 0.5 μmol/mg for the 0.025 and 0.1 M titrations presented here.

The pK_a spectrum for *Bacillus subtilis* can be compared to typical spectra for NOM. From Smith and Kramer, (*9*) the trend for NOM samples is "carboxylic" and "phenolic" sites at the extremes of the spectrum and various intermediate pK_a values in-between. The carboxylic sites are generally more acidic for NOM samples with pK_a values around 4 rather than 5 as observed for bacteria in this study. The hydroxyl sites generally show values around 10 for NOM, which is very similar to values reported here for bacteria, although as mentioned above for bacteria without phenolic structures these sites are probably better interpreted as amine sites. The total concentration of sites in NOM is reported between 4 and 24 μmol/mg NOM at 0.1 M ionic strength (*9*). The total concentration here is 0.482 μmol/mg bacteria at 0.1 M ionic strength. Thus, the site density on bacteria is less than that for NOM compared on a dry weight basis.

The site capacity can also be compared to HFO. The best estimates of site capacity presented by Dzombak and Morel (*2*) is 2.25 μmol/mg HFO, again greater than our estimate for *B. subtilis*. However, a comparison of site density per surface area reveals that the site densities are very similar. Using the HFO area estimate of 600 m^2/g (*2*) and the *B. subtillus* estimate of 140 m^2/g (*11*) yields 3.75 and 3.44 μmol/m^2 for the HFO and bacteria, respectively. The site energies for HFO are quite different though with $pK_{a1} = 7.29$ and $pK_{a2} = 8.93$ from the best estimates of Dzombak and Morel using the diffuse double-layer model (*2*). Here we have both more acidic sites and more basic sites determined for *B. subtilis*.

From the point of view of curve-fitting the data to generate predictive parameters, either the approach suggested here

or that of Fein et al. (*11*) could be used. Discrete site modeling is advantageous over continuous modeling because discrete sites are directly useable in geochemical code calculations. For electrostatic modeling, the constant capacitance parameter has little, if any, physical meaning; therefore, the conditional approach used here is recommended. The results presented here show that it is not possible to treat electrostatic effects at all sites using a single constant capacitance fitting parameter; the effects of ionic strength are not independent of pH, and higher pK_a sites have stronger electrostatic effects. This emphasizes the intrinsic heterogeneous nature of the chemical reactivity of bacterial surfaces. The close agreement between the results determined here and the results determined by Fein et al. (*11*) using independent experiments and a different modeling approach is encouraging. This implies that bacterial surfaces are sufficiently quantitatively consistent to be modeled using geochemical equilibrium calculations.

Acknowledgments

This work was supported by a Natural Sciences and Engineering Research Council (NSERC) of Canada Grant to F.G.F. We would like to thank Nagina Parmar for assistance with microbiological aspects of this project.

Literature Cited

(1) Davis, J. A.; Kent, D. B. In *Mineral−Water Interface Geochemistry Reviews in Mineralogy Volume 23*; Hochella, M. F., White, A. F., Eds.; Mineralogical Society of America: Washington, DC, 1990; p 177.
(2) Dzombak, D. A.; Morel, F. M. M. *Surface complexation modeling, hydrous ferric oxide*; Wiley-Interscience: New York, 1990.
(3) Wang, F.; Chen, J.; Forsling, W. *Environ. Sci. Technol.* **1998**, *31*, 4448.
(4) Wen, X.; Du, Q.; Tang, H. *Environ. Sci. Technol.* **1998**, *32*, 870.
(5) Jenne, E. A., Ed. *Adsorption of Metals by Geomedia: Variables, Mechanisms, and Model Applications*; Academic Press: New York, 1998.
(6) Borkovec, M.; Rusch, U.; Westall, J. C. In *Adsorption of Metals by Geomedia: Variables, Mechanisms and Model Applications*; Jenne, E. A., Ed.; Academic Press: New York, 1998; Chapter 22.
(7) Kinniburgh, D. G.; van Riemsdijk, W. H.; Koopal, L. K.; Benedetti, M. F. In *Adsorption of Metals by Geomedia: Variables, Mechanisms and Model Applications*; Jenne, E. A., Ed.; Academic Press: New York, 1998; Chapter 23.
(8) Tipping, E. *Aquat. Geochem.* **1998**, *4*, 3.
(9) Smith, D. S.; Kramer, J. R. *Environ. Int.* **1999**, *25*, 307.
(10) Beveridge, T. J., Doyle, R. J., Eds. *Metal Ions & Bacteria*; Wiley-Interscience: New York, 1989.
(11) Fein, J. B.; Daughney, C. J.; Yee, N.; Davis, T. A. *Geochim. Cosmochim. Acta* **1997**, *61*, 3319.
(12) Daughney, C. J.; Fein, J. B. *J. Colloid Interface Sci.* **1998**, *198*, 53.
(13) Daughney, C. J.; Fein, J. B.; Yee, N. *Chem. Geol.* **1998**, *144*, 161.
(14) Beveridge, T. J.; Davies, J. A. *J. Bacteriol.* **1983**, *156*, 846−858.
(15) Campbell, M. K. *Biochemistry*; Harcourt Brace: New York, 1991.
(16) Hammond, S. M.; Lambert, P. A.; Rycroft, A. N. *The Bacterial Cell Surface*; Croom Helm: London, 1984.
(17) Beveridge, T. J. In *Metal Ions & Bacteria*; Beveridge, T. J., Doyle, R. J., Eds.; Wiley-Interscience: New York, 1989; Chapter 1.
(18) Doyle, R. J. In *Metal Ions & Bacteria*; Beveridge, T. J., Doyle, R. J., Eds.; Wiley-Interscience: New York, 1989; Chapter 9.
(19) Urrutia, M. M.; Kemper, M.; Doyle, R.; Beveridge, T. J. *Appl. Environ. Microbiol.* **1992**, *58*, 3837.
(20) Hancock, I. C. In *Microbial Cell Surface Analysis*; Mozes, N., Handley, P. S., Busscher, H. J., Rouxhet, P. G., Eds.; VCH Publishers: New York, 1991; Chapter 2.
(21) Kramer, J. R.; Collins, P. V.; Brassard, P. *Mar. Chem.* **1991**, *36*, 1.
(22) Contescu, C.; Jagiello, J.; Schwarz, A. *Langmuir* **1993**, *9*, 1754.
(23) Lu, W.; Smith, E. H. *Geochim. Cosmochim. Acta* **1996**, *60*, 3363.
(24) Brady, P. V.; Cygan, R. T.; Nagy, K. L. In *Adsorption of Metals by Geomedia: Variables, Mechanisms and Model Applications*; Jenne, E. A., Ed.; Academic Press: New York, 1998; Chapter 17.
(25) Westall, J. C. *FITEQL: a computer program for the determination of chemical equilibrium constants from experimental data;* Report 82-01; Department of Chemistry, Oregon State University: Corvallis, OR, 1982.
(26) Hiemstra, T.; Van Riemsdijk, W. H. *J. Colloid Interface Sci.* **1999**, *210*, 182.
(27) Perdue, E. M. In *Organic Acids in Aquatic Ecosystems*; Perdue, E. M., Gjessing, E. T., Eds.; John Wiley & Sons: New York, 1990; pp 111−126.
(28) Robertson, A. P.; Leckie, J. O. *Environ. Sci. Technol.* **1998**, *32*, 2519.
(29) Tobler, H. J.; Engel, G. *Naunyn-Schmiedeberg's Arch. Pharmacol.* **1983**, *322*, 183.
(30) Leuenberger, B.; Schindler, P. W. *Anal. Chem.* **1986**, *58*, 1471.
(31) Brassard, P.; Kramer, J. R.; Collins, P. V. *Environ. Sci. Technol.* **1990**, *23*, 195.
(32) Černík, M.; Borkovec, M.; Westall, J. C. *Environ. Sci. Technol.* **1995**, *29*, 413.
(33) Smith, D. S.; Adams, N. W. H.; Kramer, J. R. *Geochim. Cosmochim. Acta*, in press.
(34) de Wit, J. C. M.; van Riemsdijk, W. H.; Koopal, L. K. *Environ. Sci. Technol.* **1993**, *27*, 2015.
(35) Milne, C. J.; Kinniburgh, D. G.; de Wit, J. C. M.; van Riemsdijk, W. H.; Koopal, L. K. *Geochim. Cosmochim. Acta* **1995**, *59*, 1101.
(36) Stumm, W. *Chemistry of the Solid-Water Interface*; Wiley-Interscience: New York, 1992.
(37) Stern, O. *Z. Elektrochem.* **1924**, *30*, 508.
(38) Lützenkirchen, J. *J. Colloid Interface Sci.* **1999**, *210*, 384.
(39) Plette, A. C. C.; van Riemsdijk, W. H.; Benedetti, M. F.; van der Wal, A. *J. Colloid Interface Sci.* **1995**, *173*, 354.
(40) Harris, D. C. *Quantitative Chemical Analysis*, 4th ed.; Freeman Publishers: New York, 1995.
(41) Stumm, W.; Morgan, J. J. *Aquatic Chemistry*, 3rd ed.; Wiley-Interscience: New York, 1996.
(42) Grace, A. *Matlab optimization toolbox user's guide*; The MathWorks, Inc.: Natick, MA, 1992.
(43) Perdue, M. E. In *Humic Substances in soil, sediment and water*; Aiken, R. G., McKnight, D. M., Wershaw, R. L., MacCarthy, P., Eds.; Wiley-Interscience: New York, 1985; pp 493−526.
(44) James, A. M. In *Microbial Cell Surface Analysis*; Mozes, N., Handley, P. S., Busscher, H. J., Rouxhet, P. G., Eds.; VCH Publishers: New York, 1991; Chapter 9.
(45) Martell, A. E.; Smith, R. M. *Critical Stability Constants, Vol. 1 Amino Acids*; Plenum: New York, 1974.
(46) Shenouda, N. S.; Pan, Y.; Schaefer, J.; Wilson, G. E. *Biochim. Biophys. Acta* **1996**, *1289*, 217.
(47) *CRC Handbook of Chemistry and Physics*, 47th ed.; CRC Publishers: Boca Raton, FL, 1967; p A-243.

Received for review June 2, 1999. Revised manuscript received September 14, 1999. Accepted September 16, 1999.

ES990627L